DEVELOPMENT OF A MULTI-SCALE NUMERICAL APPROACH FOR THE CRASHWORTHINESS OF EVTOL AIRCRAFTS

Edoardo Novembre, Politecnico di Milano, Milan, Italy
Antonio Maria Caporale, Politecnico di Milano, Milan, Italy
Sebastiano Di Mauro, Politecnico di Milano, Milan, Italy
Paolo Astori, Politecnico di Milano, Milan, Italy
Chiara Mirani, Volta Structural Energy S.r.l., Lomazzo (CO), Italy
Alessandro Airoldi, Politecnico di Milano, Milan, Italy

Abstract

Electric Vertical Take-off and Landing (eVTOL) vehicles have drawn the interest of companies and researchers because of their potential application in Advanced Air Mobility. However, many challenges must be addressed, one of the most important being safety. This paper presents a numerical and experimental multi-scale approach, from the Li-Ion battery level up to the integration of the energy storage system within the airframe, aimed at assisting the early design phase of crashworthy eVTOL aircraft. Various activities will be proposed to demonstrate the general approach and its capabilities, supported by preliminary yet insightful results. Key findings include the use of dummy cells for safe abuse testing, assessment of local decelerations in modules during experiments, development of battery pack protection concepts including the possible use of Na-Ion structural battery, and evaluation of energy-absorbing systems' efficiency in alleviating loads on the vehicle frame.

1. INTRODUCTION

The transition to sustainable transport will play a key role in slowing down climate change, this sector being responsible for about 24% of global carbon dioxide emissions, as reported in Ref. 1. Although according to Ref. 2 aviation contribution is relatively small, the CO_2 emissions due to air travel, freight, and military operations are steadily increasing at a rate between 4 and 5% a year. Against this background, battery-based electric vehicles represent one of the most investigated solutions for the next generation of aircrafts. A promising application for battery-based electric vehicles is all-electric and hybrid-electric vertical take-off and landing (eVTOL) aircrafts, which many Urban Air Mobility projects identified as possible candidates for Air Metro or Air Taxi services.

Despite the technical challenges, the Federal Aviation Administration's forecast FY 2024–2044 (Ref. 3) assumes an increase in daily eVTOL departures from approximately 800 in 2025 to over 10000 by 2030. It is also worthy of consideration that, as Ref. 4 argues, it is likely that eVTOLs will mainly operate on an 'on-demand' operational model, which statistically involves more accidents compared to the scheduled model adopted for instance by major airlines.

The safety of these innovative vehicles represents a new challenge for aircraft manufacturers. The need for extremely light structures emphasizes the importance of new solutions to address traditional primary crashworthiness requirements in the aircraft field, such as mass retention, occupant loads, survivable volume, and egress path. In addition, peculiar aspects related to the safety of the energy storage system must be considered in the case of an eVTOL aircraft, as stated in Ref. 5.

In Ref. 6 the risks linked to batteries are classified in two categories: the functional ones, related to the loss of safety critical power, and the thermal ones, related to excessive heat, thermal runaway or fire events. The latter have been documented during cruise, charging, taxiing and crash. This last scenario has been addressed in the last years by the automotive field: as many electric cars are already on the market, a significant database of accidents is available to define and establish adequate regulations (Ref. 7).

Hence, the environmental obstacles that eVTOL will encounter operating in constrained airspace, combined with the risks associated to batteries, make safety a challenging task that both FAA and EASA are addressing, trying to define harmonized certification requirements (14 CFR 21.17(b), Ref. 8). As highlighted in Ref. 9, full-scale crash experiments are very expensive, and it will be fundamental to develop numerical and experimental methodologies that can support the early design stage of crashworthy eVTOL aircrafts. This paper therefore presents a multi-scale framework to design crashworthy eVTOL energy storage systems by applying a system level crashworthiness approach. Such framework comprises three distinct levels of detail: (i) battery cell; (ii) battery module/pack; (iii) structural integration of the energy storage system within the airframe.

The primary goal of the paper is to develop a general approach and the relevant tools to examine the crashworthiness performance of the involved components and propose improvement solutions. Moreover, the activities described have achieved some preliminary but significant results regarding (a) the possibility of using dummy cells for a fast and safe evaluation of local decelerations inside the battery modules, (b) the development of new concepts for the protection of the battery pack, including the possible adoption of Na-Ion structural batteries to protect the main Li-Ion modules, and (c) the evaluation of the efficiency of energy absorbing systems to attenuate the loads on the vehicle frame in case of installation of energy storage systems on the cabin top. Such preliminary results will be detailed in the paper.

2. MODELLING OF LI-ION BATTERY MODULES

2.1 Development of a case study with surrogate of functional cells

Internal Short Circuits (ISC) occurring in Li-Ion cells represent one of the main risks related to the safety of electric vehicles, since they lead to thermal runaway phenomena and possible development of fire and explosions. Mechanical abuses consequent to vehicles collisions are known as one of the most frequent causes of ISC, as reported in Ref. 10. Several studies show that a well-defined correlation can be established between the possible onset of thermal runaway phenomena and the loads, as well as the deformation experienced by the cells in case of impact or shock events (Ref. 11). Therefore, the study of the crash performance of a Li-Ion energy storage system should include the analysis of the loads, decelerations, and deformation experienced by the cells in impact conditions.

Focusing on cylindrical cells, which are still one of the most adopted energy storage units in electric vehicles, this section illustrates the activity performed at the cell level with the following goals:

- developing non-functional but mechanically equivalent surrogate cylindrical cells, including accelerometers, to allow safe testing and reliable evaluation of local decelerations;
- performing impact tests on representative module elements, acquiring data regarding overall impact response and local response (decelerations and indentations) of the cells;
- developing numerical models of the representative elements to investigate the key issues in the simulation of local and global responses.

To accomplish such goals, a representative portion of a battery module, in a typical configuration used in automotive field, was fabricated using Fused Deposition Modeling (FDM) with Thermoplastic Polyurethane (TPU). This included the external structure, internal supports, and a replica of the cooling system.

The TPU element was designed to host 23 21700 Li-ion cells with a steel case, as shown in Figure 1-a. The surrogate cells used in the tests were manufactured in two versions: (i) a set of inertially equivalent cells, which were produced by filling the external shells of commercially available 21700 Li-ion cells with lead sinkers and cotton wool; (ii) a set of structurally equivalent cells, which were produced by introducing in the steel case an aluminum alloy spiral wrapped around a pin, according to the scheme shown in Figure 2, and then filling the interior of the cell with silicone rubber. The structurally equivalent dummy cells were designed to achieve a mechanical response to static indentation similar to that of the real 21700 Li-cell reported in Ref. 11.

Three dummy cells were also endowed with an internal accelerometer, in the positions shown in Figure 1-b.

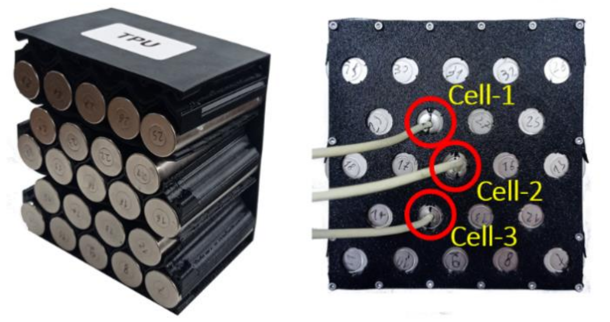

Figure 1. (a) Interior of the representative module element with Li-Ion cells (b) position of the dummy cells endowed with accelerometers

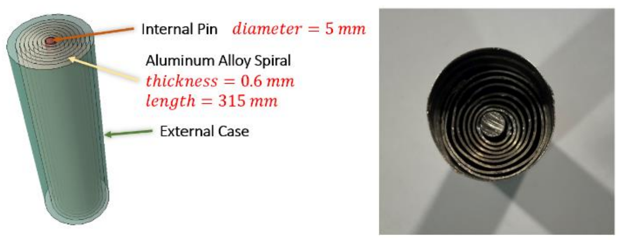

Figure 2. Scheme and accomplishment of structurally equivalent dummy cell

2.2 Experimental results

The representative module elements were subjected to impact tests using a drop tower equipped with a 100 mm diameter semispherical impactor, with a total mass of 9.3 kg. A series of tests at increasing drop height was conducted by using modules endowed both with the inertially equivalent cell (result set 1) and with the structurally equivalent cell (result sets 2 and 3) with damaged cells being replaced after each test. As shown in Figure 3, the hemispherical head impacted the top of the representative module producing a significant deformation of the TPU structure, which did not undergo permanent deformation thanks to its peculiar mechanical response.

During these impacts, the deceleration of the impactor and the three accelerometer-equipped cells was recorded. This data provided insights into both the overall structural response and the deceleration experienced by individual cells, allowing for a global-to-local correlation.

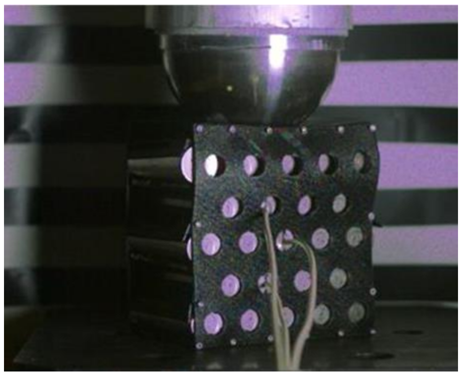

Figure 3. Drop-Tower impact test

In Figure 4, the results related to the impactor deceleration are reported for the different test sets in impact conditions characterized by a drop height of 150 mm, 350 mm, and 500 mm. The different mechanical response of cells influenced the deceleration and, as a consequence, the level of forces transmitted to the representative elements.

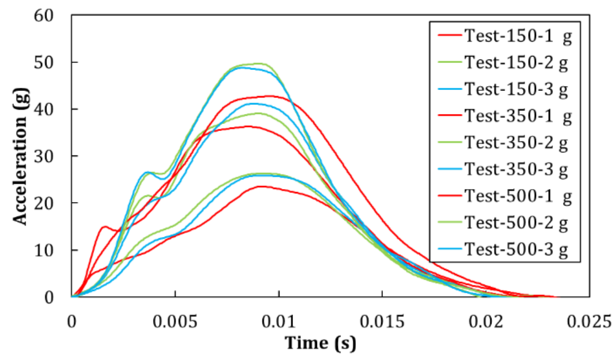

Figure 4. impactor deceleration response in the test set 1 (with inertially equivalent cells) and in test sets 2 and 3 (with structurally equivalent cells)

The local decelerations experienced by the cells are exemplified in Figure 5, referred to the test set 1. It can be observed that the local deceleration increases with the drop height, with a trend that is not completely aligned with that of the impactor deceleration. Moreover, the deceleration experienced by the cells decreases systematically with the distance from the impact point. In the results obtained with the structural equivalent cells, the measured local decelerations were generally higher than those with inertially equivalent cells (from 10% to 45%), but the same trends were observed.

The deformed cells were extracted from the module element in each test, and the maximum indentation was measured. The results of these measures for the tests performed with 150 mm, 350 mm, and 500 mm drop heights are reported in Figure 6.

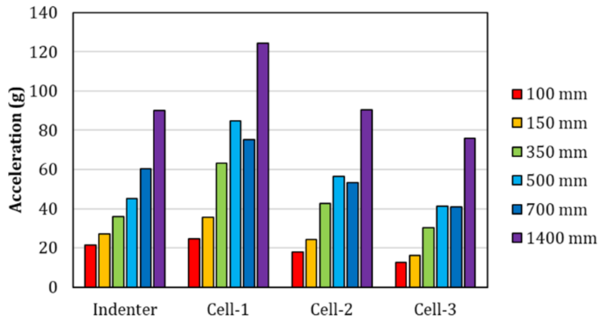

Figure 5. Impactor and cell deceleration in the tests performed with inertial equivalent cells

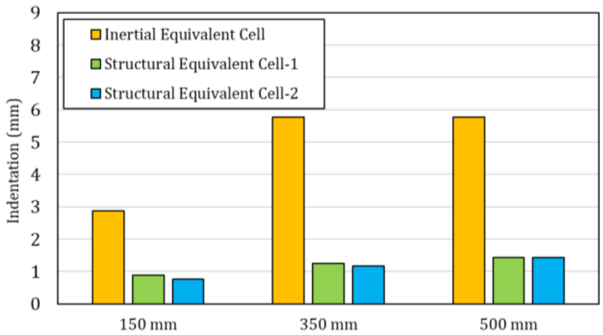

Figure 6. Maximum indentations experienced by the cell cases

In terms of maximum indentation, a noticeable difference exists between the two types of cells. In general, it can be noticed that indentation occurs even in the tests with a low impact energy. Although these results are significantly influenced by the particularly compliant material used for the structure of the representative module element, it can be stated that, when the structure of the module case is deformed, cells experience local decelerations and indentations that depend on the distance from the impact points and on their mechanical responses. The test method based on the equivalent cell can be adopted to identify the most critical positions and to design improved internal structures to mitigate the loads experienced, thus reducing the risk of ISCs phenomena.

2.3 Numerical model and correlation at the local and global level

A numerical model of the drop tower tests performed with the inertially equivalent cells was developed using the Simulia/Abaqus explicit code, replicating the physical tests (Figure 7). In the models the structure of the TPU module, of the cooling system, and of the steel cells were represented by shell elements, while the internal filler of the cells was modelled by hexahedral elements.

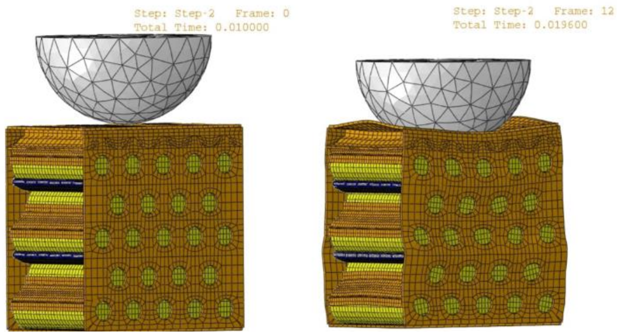

Figure 7. Undeformed and deformed module during the impact simulation with inertially equivalent cells

During the model tuning phase, careful attention was given to the material constitutive laws and the contacts within the module. The cells' external shells were modeled using an elastoplastic law, the Thermoplastic Polyurethane (TPU) was represented with a Prony series-based viscoelastic law, the cooling system was modeled with an Ogden hyperelastic law, and for the cells' internal jelly roll the **Crushable Foam* model available in the software (Ref. 12) was used. Various methods were explored to simulate the axial pressure exerted by the module walls on the cells, including a general contact algorithm and a fictitious thermal expansion applied to beam elements representing the screws.

A good numerical-experimental correlation was achieved for the indenter deceleration, as shown in Figure 8.

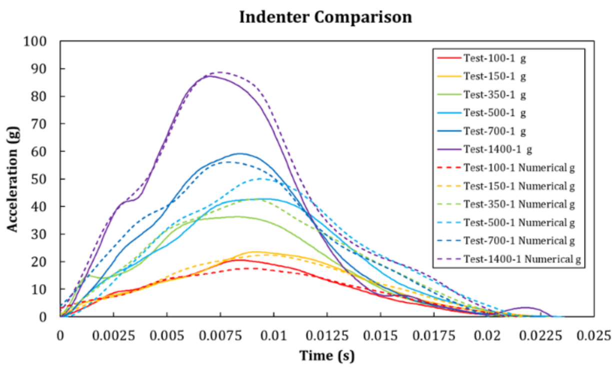

Figure 8. Numerical-experimental correlation for the deceleration experienced by the indenter

The local deceleration experienced by the cells was found sensitive to the fine tuning of the TPU material model and to the properties of contact interactions between the different parts of the models, including contact friction. The level of correlation achieved is summarized in Figure 9, where the peak deceleration obtained in the time histories filtered at 180 kHz is compared with the experimental results.

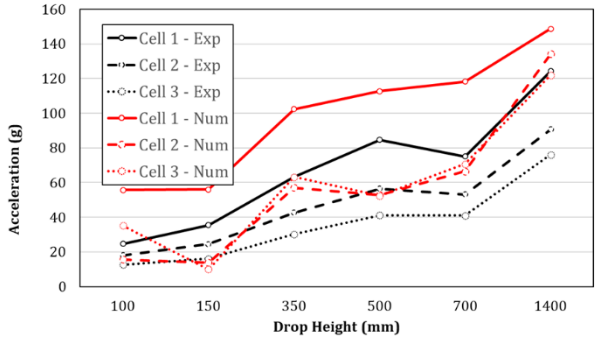

Figure 9. Numerical-experimental correlation for the local decelerations experienced by the cells endowed with accelerometers

Considering the difficulties of model characterization and the complexity of the interactions between the different part of the representative module element, the result presented in Figure 9 can be deemed satisfactory, since the increment of deceleration peak with the drop height and the decrease with the distance for the impact point are qualitatively captured. Quantitatively, major errors can be observed for cell 1, which was closer to the impact point. Despite such quantitative discrepancies, the correlation referred to the maximum indentation is appreciable both from the quantitative and qualitative point of view, as shown in Figure 10.

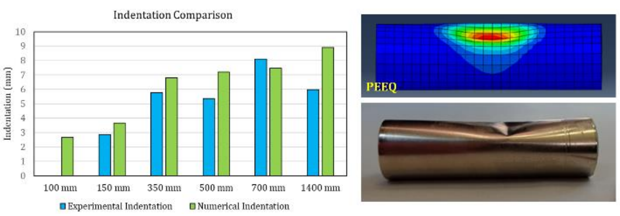

Figure 10. (a) Quantitative and (b) qualitative numerical-experimental correlation for the indentation experienced by the cells

Overall, the results pointed out the difficulties for a correct prediction of the local deceleration and loads experienced by the energy storage units and the need of carefully performed calibration tests to obtain reliable models.

3. PROTECTION CONCEPTS FOR ELECTRIC AIRCRAFT BATTERIES

3.1. Aluminum foam absorbers concept

This section considers a battery pack with Li-Ion cells embedded in five modules with an aluminum case. Modules are structurally connected by an aluminum flange and a carbon fiber composite case encloses all the pack. The investigated scenario is a drop test from 15.2 m (EASA Moc SC-VTOL 2, Ref. 13). The pack may have a generic installation in the eVTOL aircraft, considering that Ref. 13 indicates that the test can be performed on the energy storage system including part of the surrounding structure. Hence, the objective of this study is to design and assess a passive energy absorber by means of FE analysis that can minimize the deceleration experienced by the modules in the considered impact conditions. During the activity, the measured index was the average acceleration of the material representing the cells integrated inside the module, which is not modeled in detaill. The selected material for the energy absorbing structure is aluminum foam, due to its excellent Specific Energy Absorption (SEA) and because it can be easily shaped into the desired geometry. Moreover, aluminum foams with densities varying from 400 to 1200 kg/m^3 are available on the market, and this provides the possibility of tuning some of the mechanical properties according to the specific requirements, as described in Ref. 14. Additionally, aluminum foam does not have a preferred direction for energy absorption performances and may work in impacts with different attitudes.

It is worth noting that the volume available for the installation of a passive absorbing system was kept limited to consider a realistic design configuration. In particular, the available stroke between the bottom of the module cases and the composite case of the pack was fixed to just about 30 mm. Such a condition is particularly challenging to limit the deceleration of the modules.

The FE analyses were run by using the Abaqus/Explicit code. Within the simplified model of the battery pack, the cells are represented by a mesh of uniform hexahedrons made of a compliant isotropic material, whose main role it to grant the required inertia. The model can be considered representative of a module based on pouch cells, which do not comprise an external structural case at the cell level. Therefore, the stiffness of the module is supplied exclusively by their external aluminum case. The aluminum parts were modelled by shell elements and an elastic-plastic law with perfect plasticity was implemented. The composite case was modelled by shell elements with an orthotropic elastic law including an Hashin failure criterion calibrated through available test data. Finally, the aluminum foam was modelled by solid 8-noded elements embedding the *C*rushable Foam* behavior with isotropic hardening that is available in the software code. After the elastic regime, the stress-strain response of the material is characterized by a plastic plateau followed by the hardening stage, which effectively captures the densification phenomenon that is typical of metallic foams. Moreover, the Cowper-Symonds law was included to grasp the strain-rate sensitivity of the material. The required parameters for the material card, including the ones for the Cowper-Symonds law, were obtained from Ref. 15.

An estimate of the required crushing force was provided by assuming the available maximum stroke of about 30 mm and by considering an ideal response with unit load uniformity ratio. Different configurations were examined before selecting the final one. The first design involved just lateral absorbers, as shown in Figure 11-a. However, according to the FE simulations, this configuration involves local buckling of the corners of the absorber, which prevents the correct crushing mechanism of the overall structure. To better support the modules and decrease the free bending span, discontinuous central absorbers were added to the battery pack (Figure 11-b). The attempt was nevertheless unsuccessful, since the peak accelerations increased.

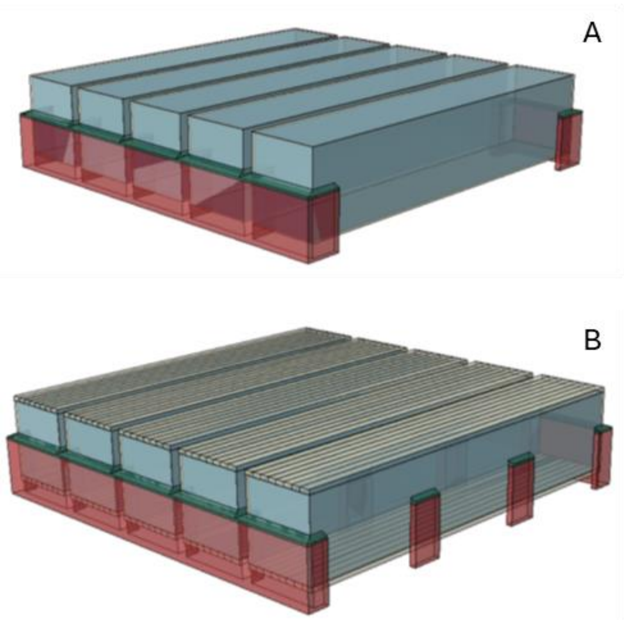

Figure 11. Discarded solutions with discontinuous foam absorber

Eventually, the solution illustrated in Figure 12 was found to be the best. The aluminum flange connects the modules and transfers the load to the foam absorber, which provides a distributed crushing stroke before contact with the composite case occurs. The absorber is a continuous structure that runs through all the modules, guaranteeing an adequately controlled crushing response. Moreover, the fact that the foam is not placed directly under the modules, but rather connected to their lateral surface, make possible the exploitation of all the available stroke without the limitation imposed by the foam densification, which typically occurs at 60% of engineering compressive deformation. The key geometric parameters of the battery pack are listed in Table 1.

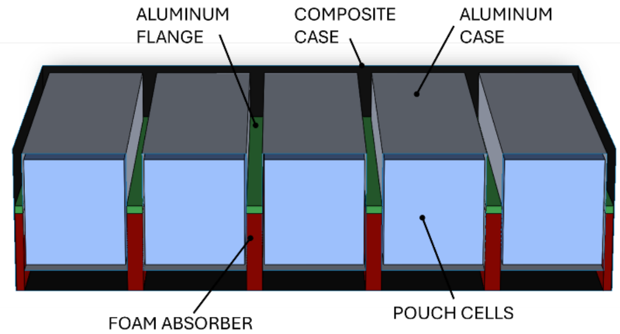

Figure 12. View cut of the selected geometry for the battery pack

Table 1. Key geometric parameters of the battery pack

Component	Dimension	Value
Modules	Length	950 mm
	Width	160 mm
	Height	190 mm
	Thickness	1.5 mm
	Number	5
Absorber	Stroke	33 mm
	Width	25 mm

The configuration shown in Figure 12 acted as a baseline for a sensitivity analysis focused on the peak of acceleration measured on the pouch cells during the drop test. The simulations were carried out by modeling just a quarter of the pack, since multiple analyses were anticipated. The typical time history of the equivalent rigid-body vertical acceleration of the cells is shown in Figure 13. This output was directly provided by the solver (Ref. 12) and the response was then filtered with a SAE600 filter. In Figure 13, the first peak indicates the moment of the impact, which is followed by the dumped oscillations of the cells. The most solicited module is the one in position 2, whereas the one in position 1 experiences a rebound before reaching the maximum acceleration. Figure 13 also illustrates the contour of the equivalent plastic strain in the aluminum foam, which highlights how the compression of the lower part of the absorber dissipates the impact energy.

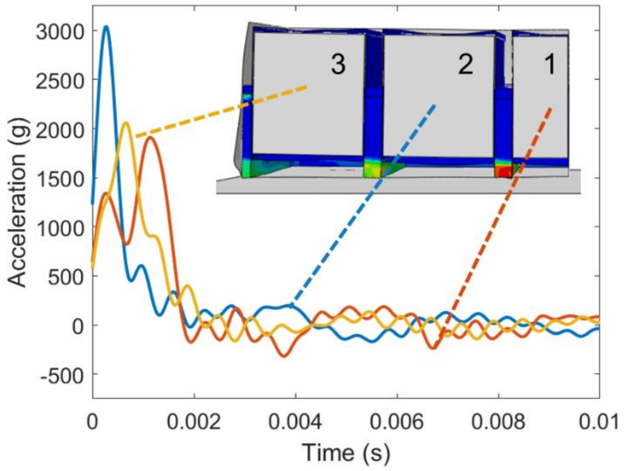

Figure 13. Filtered time history of cells' vertical acceleration

In the sensitivity analysis, the investigated parameter was the density of the aluminum foam. Results shown in Figure 14 indicate that the best solution is resorting to a low-density foam for the absorber, in the range between 400/500 kg/m^3. This is because with low density foams the stroke is almost completely exploited. As shown in Figure 14, the best solutions achieved an improvement of the peak acceleration of about 50% with respect to the worst design, proving that the proposed energy absorbing system can effectively absorb the impact energy. It is worth noting that, in the investigated range, the peak acceleration of module 2 is linearly linked to the foam density.

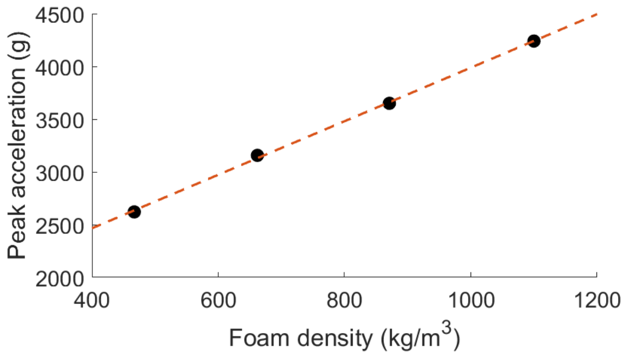

Figure 14: Filtered time history of cells' vertical acceleration

3.2. Concept based on structural battery

3.2.1. Volta SE structural battery

A recent technological solution provided by Volta SE company makes available a structural battery based on Na-Ion electrochemistry. The structural battery is realized by exploiting the architecture of sandwich panels. As shown in Figure 15, panels are made of a thicker central layer (the core) and two thinner, more rigid, outer layers (the skins). The energy storage capability is provided by the core that hosts the active materials. The core is realized through a series of corrugated Na-Ion electrochemical cells, attached together to form a honeycomb-shaped structure.

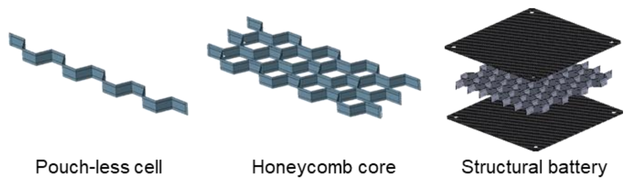

Figure 15. Main components of the structural battery by Volta SE

The developed electrochemical cells differ from the standard commercial pouch cells not only by the 3D corrugated shape, but also by the absence of the pouch lining that contains the electrodes' arrangement (called pouch-less configuration). The pouch-less cells can be manufactured in various geometries, including different corrugation shapes, lengths, and widths. These cells are bonded together using a low temperature curing epoxy to create a honeycomb core (see Figure 16-a). The tabs are then welded according to the desired connection scheme to achieve the required voltage and amperage at the pack level.

The term Structural Battery Panel (SBP) refers to the entire sandwich panel, as illustrated in Figure 16-b. The pouch-less cells can be organized into groups (or modules) within the sandwich panel. The choice of connection type for both the pouch-less cells within a module and the modules themselves depends heavily on the application's geometrical, structural, and electrical requirements. The skins of the SBP require at least an electrical insulation layer on the internal side of the skin to prevent the pouch-less cells from short-circuiting. The choice of the lamination sequence of the skins depends on structural, thermal and cost requirements. The SBP can be enhanced with structural reinforcement ribs to improve its structural performance and ensure a proper mechanical connection with the system to which it will be attached.

The SBP can be produced in planar, single or double curvature panels. There is no virtual limitation on the dimensions of the SBP, considering that the manufacturing process is based on the standard manufacturing process of sandwich composite panels.

Concerning the thickness of the SBP, a minimum of 10 mm is advised to have a decent mass ratio between active materials over inert SBP mass. Indeed, a low concentration of active materials results in a reduced energy density for the SBP. Actually, the SBP design is agnostic from chemistry: any active material can be coated onto the electrodes. Currently, the SBPs architecture incorporates state of the art Na-ion chemistry, a strategic emerging electrochemical technology leveraging on low costs, abundant materials and a simpler supply chain.

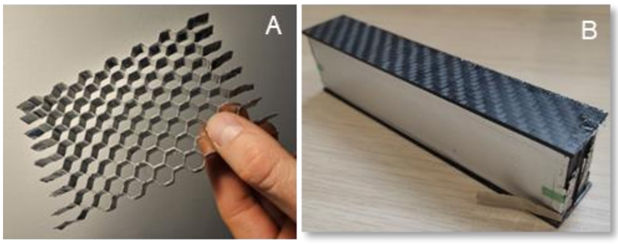

Figure 16. (a) Example of produced active core; (b) Structural Battery Panel with carbon fiber skins.

In the proposed application, the SBP configuration and the Na-Ion electrochemistry are exploited to design an additional protective layer for the modules introduced in the previous sub-section. Indeed, the Na-Ion battery are not subjected to the risk of fire and explosion in case of ISC, and this makes possible conceiving a configuration where the SBP panel is crushed providing energy absorption performance analogous to the one of a conventional sandwich panel. From the functional point of view, the energy density of the whole pack will be increased thanks to the energy stored in SBP.

3.2.2. Integration of structural battery within the protection system

To investigate the potential performance of the additional SBP in the pack configuration considered in Section 3.1, an external layer of structural battery with a thickness of 30 mm was included at the bottom of the composite case. For simplicity, the honeycomb was modelled as a homogenized material by using the **Crushable Foam* card with the adequate constitutive properties taken from Ref. 16. Considering a 1/8” cell size and a nominal density of about 100 kg/m^3, the modulus was fixed to 3 GPa and the crushing strength to 3.1 MPa. Given the previously presented results, the aluminum foam absorber was characterized by a density of 500 kg/m^3.

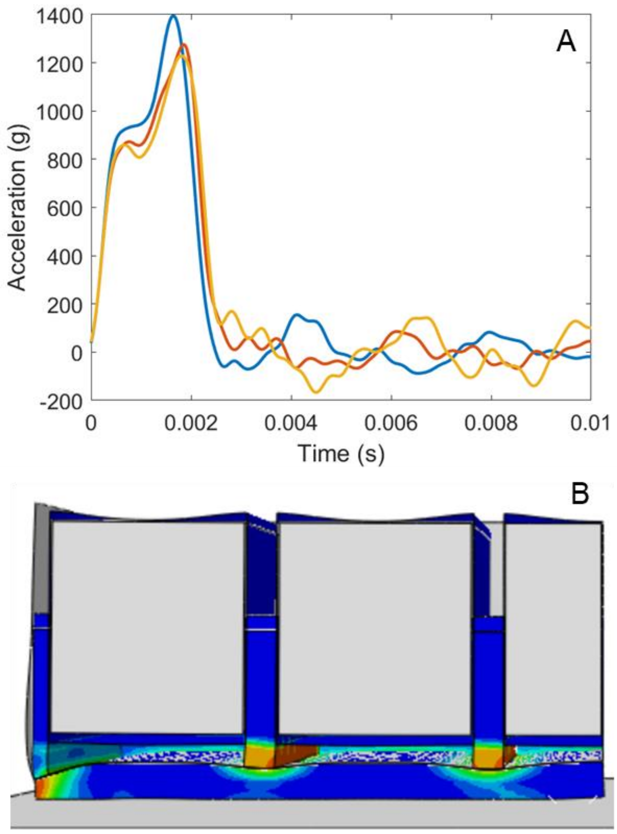

Figure 17. (a) Filtered time history of cells’ vertical acceleration; (b) Plastic equivalent strain in foam and structural battery absorbers.

As expected, the additional absorber significantly reduced the acceleration experienced by the cells (see Figure 17-a). The acceleration profile is smoother and spread over a longer time span, and the maximum value was roughly halved. Figure 17-b illustrates that the honeycomb and foam absorber work together effectively: the upper structure transfers the load to the structural battery, which then experiences plastic deformation under compressive loading granting additional stroke.

Considering the whole battery pack, the aluminum foam absorber represents 6.4% of the mass, and the structural battery 1.0%. This preliminary study shows that the structural battery can both store extra energy and provide significantly improved crash protection for the main battery pack.

4. HYBRID FEM-MULTI BODY PLATFORM FOR CRASHWORTHINESS SYSTEM LEVEL APPROACH

At the level of the whole eVTOL structure, the goal of the proposed multi-scale approach is to investigate the integration of the crashworthy battery pack into the airframe in the early design stage. This implies a large number of simulations, and therefore the need for computationally efficient tools. For this reason, FE and multibody techniques were joined to develop a hybrid numerical platform for an eVTOL cabin. This solution allows to significantly reduce the computational time required by the analyses while retaining an adequate level of reliability.

The key components of the platform are: (i) the hybrid model of the cabin airframe; (ii) the hybrid model of the seats and the Anthropomorphic Test Devices (ATDs); (iii) the model of the battery pack. The assembly is shown in Figure 18, where an installation of the energy storage system on the top of the cabin was considered.

In this case, the cabin model comprises the subfloor, the floor, the cabin roof and three fuselage frames, which are connected to the lateral bulkheads of the subfloor. Being the focus on the crash response of the eVTOL structure, the subfloor plays a key role. An energy absorbing subfloor configuration was adopted on the basis of the solutions presented by Ref. 17 for helicopters. The aluminum skin of the subfloor is modelled with shell elements, as well as lateral bulkheads and the keel beams. The intersection elements, which act as energy absorbing elements in vertical crashes, are represented by 2-noded connector elements with an elastic-plastic response coupled with a plasticity driven damage (Ref. 12). The geometry of the subfloor and the position of the connector elements is illustrated in Figure 19. The floor was meshed by solid and shell elements to simulate a sandwich plate. The frames of the cabin shown in Figure 18 are modelled with beam elements and have an I-beam section that was sized considering a 30 g load. For simplicity, the roof was modelled with a rigid plate.

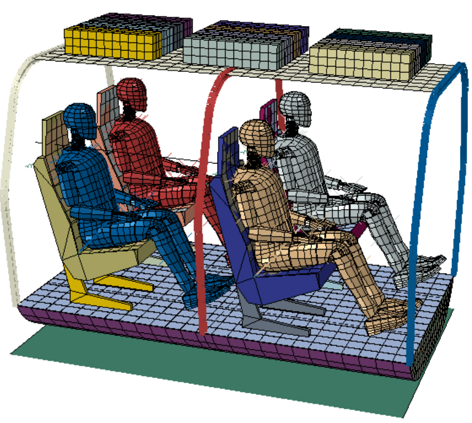

Figure 18. Numerical hybrid platform of the eVTOL cabin

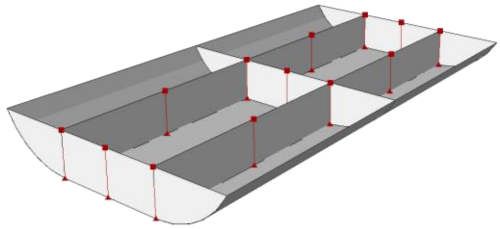

Figure 19. Geometry of the subfloor with highlighted connectors

The models of the seats and ATDs combine FE deformable elements together with rigid parts, springs, connectors and lumped mass elements. The numerical ATDs and seats were developed in previous works presented in Ref. 18 and Ref. 19. In the present work, the architecture of the model was modified to ease the implementation of multiple ATDs within the cabin model, and the absorber of the seat was calibrated to achieve compliance with the regulations prescribed in Ref. 20 in terms of maximum lumbar load.

Finally, a simplified model of the battery pack was included in the platform. The mass of the modules is distributed in the hexahedrons placed on the cabin roof. The connection was made by means of connector elements.

The whole model exemplifies a numerical approach that can be used in early design phases to study optimal crashworthy configurations. The preliminary results that are reported in the following represent analyses that were conducted with a specific aim. In particular, the effect of installing an energy absorbing system in the battery pack was investigated, considering the alleviation of the loads exerted on the frames by the battery pack inertia.

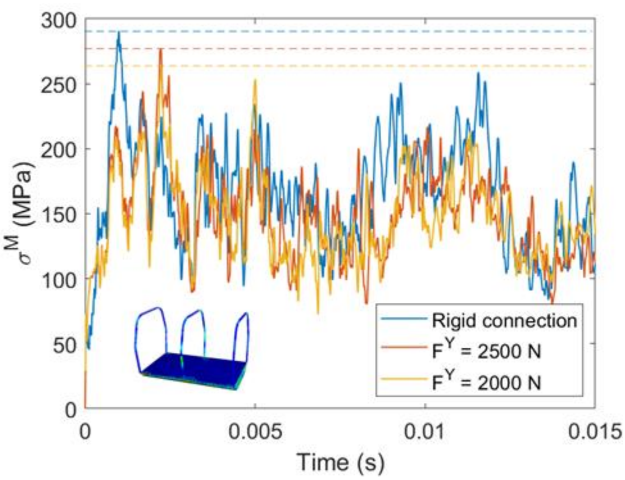

Figure 20. Stress envelope of the frames during the crash analyses with different connector behavior

At first, all the relative degrees of freedom of the connectors were blocked to model a rigid connection between the cabin roof and the mass of the modules. Then, in the second and third case, the connectors behavior was defined as an elastic plastic law with two different yielding force: 2500 and 2000 N, respectively. The equivalent Von Mises stress in the beam elements of the frame was monitored, so to compute the maximum stress envelope during the analyses for the three investigated scenarios. The stress envelope, i.e. the maximum Von Mises stress in the frames for each sampling, is illustrated in Figure 20.

The load alleviation predicted by this rather simple model is remarkable. The maximum Von Mises stress in the case of rigid connection is 290 MPa, which is reduced by 5% and 10% with F^Y equal to 2500 and 2000 N. The available stroke is 34 mm. With F^Y = 2500 N, the exploited stroke is 8 mm, whereas with F^Y = 2000 N it increases to 16 mm. This relatively small stroke is enough to provide this load mitigation. The stress peak, which occurs soon after the impact with the ground, is shifted in a later stage and reduced by the energy absorbing system. Further analyses with even lower yielding forces for the connectors proved that, if bottoming occurs, most of the beneficial effect get lost. This means the energy absorbing system must be carefully calibrated to both protect the energy storage system and possibly alleviate the loads on the airframe.

5. CONCLUSIONS

The paper presented a multi-scale approach dedicated to the crashworthiness of innovative eVTOL aircraft. Some preliminary results were provided and the main findings can be summarized in the following points:

1. The impact test with mechanically and inertially equivalent cells showed that cells are subjected to local decelerations and indentations that, other than their mechanical properties, also depend on their position within the module. The availability of finely calibrated numerical model could be used, for instance, to design specific internal solutions to protect the most critical areas. The adoption of dummy cells with structural equivalent properties may be particularly interesting to reduce the cost and the risk of the calibration and validation tests to be performed. Indeed, the development of a FE model highlighted the difficulties in catching the local phenomena, which highly depend on the interaction between all the involved parts and on the detailed description of material responses. However, the global behavior, the indentation of the cells and the main trends were adequately captured in the example provided.
2. A proper installation of metallic foam absorbers can be effectively used to protect the battery pack and reduce the decelerations experienced by the cells inside the modules, despite, in general, the available stroke is quite limited.
3. The preliminary analyses that were presented also suggest that the innovative SBP technology with Na-Ion chemistry is extremely promising: SBPs can increase the specific energy of the whole system by storing energy in a structure that can serve as a passive absorber for the main energy storage system.
4. According to the hybrid model of the cabin, if the battery pack is mounted on the cabin top the dynamic response of the battery pack equipped with energy absorbers can be designed so to alleviate the loads on the airframe. The energy absorbers installed in the energy storage system can therefore be relevant not only to protect the battery pack, but also for the primary crash requirements of the eVTOL aircraft such as survivable space and mass retention.

Author contact:

Edoardo Novembre, edoardo.novembre@polimi.it
Antonio Maria Caporale, antoniomaria.caporale@polimi,it
Sebastiano Di Mauro, sebastiano.dimauro@polimi.it
Paolo Astori, paolo.astori@polimi.it
Chiara Mirani, chiara.mirani@voltase.energy
Alessandro Airoldi, alessandro.airoldi@polimi.it

6. ACKNOWLEDGMENTS

This study was carried out within the MOST - Sustainable Mobility National Research Center and received funding from the European Union Next-Generation EU (Piano Nazionale di Ripresa e Resilienza (PNRR) - Missione 4. Componente 2, Investimento 1.4 - D.D. 1033 17/06/2022, CN00000023). This manuscript reflects only the authors' views and opinions, neither the European Union nor the European Commission can be considered responsible for them.

REFERENCES

[1] Solaymani, S., "CO2 emissions patterns in 7 top carbon emitter economies: The case of transport sector," *Energy*, Vol. 168, Feb. 2019, pp. 989–1001. DOI: https://doi.org/10.1016/j.energy.2018.11.145.

[2] Friedlingstein, P., et al., “Global Carbon Budget 2019,” *Earth System Science Data,* Vol. 11, Dec. 2019, pp. 1783–838. DOI: https://doi.org/10.5194/essd-11-1783-2019.

[3] Schaufele, R., and Lukacs, R., “FAA Aerospace Forecast Fiscal Years 2024–2044,” Forecast and Performance Analysis Division (APO-100), 2024.

[4] Littell, J., “Challenges in Vehicle Safety and Occupant Protection for Autonomous electric Vertical Take-off and Landing (eVTOL) Vehicles”, AIAA Propulsion and Energy 2019 Forum, Indianapolis, IN, August 2019.

[5] Waimer, M., Schatrow, P., Lützenburger, M., “Simulation Studies on eVTOL Crashworthiness in the Conceptual and Preliminary Design Phase,” Tenth Triennial International Aircraft Fire and Cabin Safety Research Conference, Atlantic City, New Jersey, October 2022.

[6] Sripad, S., Bills, A., Viswanathan, V.. “A review of safety considerations for batteries in aircraft with electric propulsion,” *MRS Bulletin*, Vol. 46, June 2021, pp. 435–42. DOI: https://doi.org/10.1557/s43577-021-00097-1.

[7] Chombo, V., P., Laoonual, Y., Wongwises, S., “Lessons from the Electric Vehicle Crashworthiness Leading to Battery Fire,” *Energies,* Vol. 14, Aug. 2021, pp. 4802. DOI: https://doi.org/10.3390/en14164802.

[8] 14 CFR 21.17(b), https://www.faa.gov/aircraft/draft_docs/ac.

[9] Caputo, F., Lamanna, G., Perfetto, D., Chiariello, A., Di Caprio, F., Di Palma, L., “Experimental and Numerical Crashworthiness Study of a Full-Scale Composite Fuselage Section,” *AIAA Journal,* Vol. 59, Feb. 2021; pp. 700–18. DOI: https://doi.org/10.2514/1.J059216.

[10] Wang, W., Yang, S., Lin, C., Shen, W., Lu, G., Li, Y., Zhang, J., “Investigation of mechanical properties of cylindrical lithium-ion batteries under dynamic loading,” *Journal of Power Sources,* Vol. 451, March 2020. DOI: https://doi.org/10.1016/j.jpowsour.2020.227749.

[11] Li, W., Xia, Y., Chen, G. H., Sahraei, E., “Comparative study of mechanical-electrical-thermal responses of pouch, cylindrical, and prismatic lithium-ion cells under mechanical abuse,” *Sci China Tech Sci*, Vol. 61, Sept. 2018, pp. 1472–1482. DOI: https://doi.org/10.1007/s11431-017-9296-0.

[12] SIMULIA Abaqus Documentations. Dassault Systèmes Simulia Corp., 2021.

[13] “Means of Compliance with the Special Condition VTOL,” EASA MOC SC-VTOL Issue 2, 2021.

[14] Simancik, F., Jerz, J., Kováčik, J., Minár, P. “Aluminium foam - A new light-weight structural material,” *Kovove Materialy,* Vol. 35, (4), Jan. 1997, pp. 265-277.

[15] Zhao, Y., Ma, C., Xin, D., and Sun, M., “Dynamic mechanical properties of closed-cell aluminum foams with uniform and graded densities,” *Journal of Materials Research*, Vol. 35, (19), Oct. 2020, pp. 2575–2586. DOI: https://doi.org/10.1557/jmr.2020.157.

[16] Hexcel Product Data Sheet, https://www.hexcel.com/Resources/DataSheets/Honeycomb. Accessed July 2024.

[17] Bisagni, C., “Crashworthiness of helicopter subfloor structures,” *International Journal of Impact Engineering*, Vol. 27, Feb. 2002, pp. 1067–1082. DOI: https://doi.org/10.1016/S0734-743X(02)00015-5.

[18] Lanzi, L., Airoldi, A., Astori, P., Grassi, F. “Optimization of energy absorbing subsystems for helicopter vertical crashes,” 25th international congress of the aeronautical sciences (ICAS 2006), Hamburg, Germany, Sept. 2006.

[19] Cacchione, B., Airoldi, A., Astori, P., “Modelling technique to optimise energy absorption in helicopter crashes,” 6th international KRASH users’ seminar (IKUS6), Stuttgart, Germany, June 2009.

[20] 14 CFR 27.562, https://www.ecfr.gov/current/title-14/section-27.562.